

International Conference on Computational Science, ICCS 2011

Numerical Investigation of Melt Segregation Using FEM Coding Environment Escript

Arash Mohajeri¹, Hans Muhlhaus, Yaron Finzi, Lutz Gross

*Earth Systems Science Computational Center, School of Earth Sciences,
The University of Queensland, St. Lucia, QLD 4072, Australia*

Abstract

Understanding of melt segregation and extraction is one of the major outstanding problems of melting processes in Earth's mantle. The volcanoes that lie along the Earth's tectonic boundaries are fed by melt that is generated in the mantle. However, it still remains unclear how this melt is extracted and finds its way towards the volcanoes. Two important mechanisms in melt segregation and migration are reactive fluid flow and mechanical shear. Reactive fluid flow describes the formation and segregation/migration of melt significantly affected by chemical interaction between melt and rock. This reactive-infiltration instability results in melt fingering which eases the transition from porous to channelized flow and provides a key element in some of the geological phenomena on earth. The second important mechanism in melt migration is localization due to mechanical shear. Recent studies have shown that when partially molten rock is subjected to simple shear, bands of high and low porosity are formed at a particular angle to the direction of maximum extension. Thus melt distribution is also influenced by stresses in partially molten rock [2,3]. The main aim of this paper is to identify the main mechanisms inducing melt segregation and effective flow. More specifically we investigate the melt reaction instability and melt band formation in this study. Here, in addition to providing a better understanding of melting phenomena in the mantle, we also develop a numerically validated model which can be used as an active and open source for future more complicated studies. For the melt bands problem, we employ the equations of magma migration in viscous materials which was originally derived by McKenzie (1984), and for the fingering instability problem we refer to the well known equations of reactive transport [4]. We write two different numerical codes using the FEM environment "escript". We test the codes for a set of well-understood case problems which have been studied previously by other researchers.

Keywords: Melting, Fingering instability, Melt bands, Shear localization, Numerical modeling, Finite element, Escript

1. Introduction

Melting in the mantle is a complex process which produces variable amounts of melted material of different mineral composition depending on the conditions during the formation. The earth's mantle melting occurs mostly at

¹Corresponding author. Tel.: +61-7-334-641-03; fax: +61-7-334-641-34.
E-mail address: arash.mohajeri@uqconnect.edu.au

the edge of the lithospheric plates and in plumes, which normally undergo intense deformations. The melt-migration mechanism in Nature is controlled by a range of driving forces. Pressure gradient (caused by shear deformation of a partially molten rock) is an example of these driving forces. Formation of high-permeability regions (fingering) and melt-enriched channels during viscous deformation of partially molten rock are responses to melt migration mechanisms [1]. Resulting melt flow patterns have great implications to volcanic eruptions, sea-floor volcanism and other processes related to plate-tectonics.

Many researchers have employed field studies, laboratory experiments, theoretical and numerical method to provide better understanding of dynamics and kinetics of melt segregation in the earth's mantle. The earliest studies of the coupling between melt transport and rock deformation in the 1970s investigated the melt migration through the mantle in buoyancy-driven fractures (Weertman 1971) and by porous flow (Ahern & Turcotte 1979) [5,6]. Those studies were followed by the important research of McKenzie in 1984. He studied the generation and compaction of partially molten rock, suggesting a new set of governing equations for the motion of the melt and rock matrix. These equations are in fact are all connected to each other by porosity, viscosity and melt velocity [4].

However, for the first time, in 1989, Stevenson showed that partially molten material segregates into high and low porosity regions. He observed that the viscosity of the solid matrix is a decreasing function of porosity when the matrix is subjected to pure shear. He identified this phenomenon as the possibility of channel formation by stress-driven melt segregation [7]. Similar to Stevenson, some other researchers argued that instability develops as a result of the dependence of rock viscosity on melt fraction (porosity). More recently, Holtzmann et al. (2003) presented experiments in which partially molten ductile rocks were deforming when subjected to simple shear [2]. The latest important study by Katz et al. (2006) successfully employed experimental and numerical methods to investigate the dynamics of melt and shear localization in partially molten rocks [8].

Moreover, some other papers explained channel formation by a reactive infiltration instability mechanism (Daines & Kohlstedt 1994; Aharonov et al. 1995, 1997) [9,10,11]. As a pioneer, Aharonov et al. (1995) employed linear analysis and showed that, in the presence a solubility gradient, the flow in a chemically reactive porous medium is unstable (e.g., adiabatic ascent of melt underneath mid-ocean ridges). They demonstrated that the initially homogeneous flow produces elongated high-porosity fingers that act as conduits for transport of fast flowing melt. This instability arises due to a positive feedback mechanism by which a region of slightly higher than average in porosity causes increased influx of unsaturated flow, leading to increased dissolution which further reduces the porosity [11]. Thus the infiltration instability (fingering instability) develops due to positive feedback between dissolution and melt percolation. The fingering instability amplifies local perturbations in melt distribution and thus in permeability. Fingering instability is a mechanism for melt flow localization which is independent of thermal and solidification effects. Fingering explains geological phenomenon such as regularly spaced volcanic features above subduction zones [12].

With all the studies undertaking to tackle the difficulties of the melting problem, there is still an obvious need for a simple numerical model which can describe the generation of partially molten rocks, and the separation of the melt from the residual solid. Such a model must be able to effectively solve the differential equations which describe the generation and extraction of magma. The principal aim of this paper is to propose such a numerical code and to obtain some solutions for particularly simple cases which could be assed analytically. For this reason the governing equations are simplified in our numerical model, however the codes can be easily modified to simulate more complicated cases.

In the present paper, we investigate both reactive melt infiltration and stress-driven melt segregation which produce melt-enriched, high-permeability channels that isolate the melt phase from the solid residuum, allowing chemical disequilibrium to exist between the ascending magma and the host rock. For fingering instability, we use the common governing equations of in-situ leaching, and for stress-driven segregation we employ the equations of magma migration in viscous materials as originally suggested by McKenzie [4].

We present a few well-understood case problems in order to have a useful benchmark for developing and testing new computer codes. We write a code in the FEM environment escript for each case problem. The boundary conditions are defined according the previously cited studies. We start with the fingering instability problem which in fact is coupled problem between reactive transport, Darcy's and porosity-permissibility equations. Later in the paper we discuss the influence of deformation on melt-extraction processes. We solve a coupled equation between deformations and melt distribution. We show that melt distribution is dependent on deviatoric stress in a viscously

deforming partially molten rock; and also, when subjected to simple shear, the coupling can lead to production of melt-enriched shear zones at various length scales.

2. Mathematical Equations

In the following we give a brief outline of the equations governing fingering instability and melt segregation.

2.1. Reactive transport governing equations

In porous media, pore fluid flow eases the chemical dissolution of minerals and is usually accompanied by a phenomenon called infiltration instabilities. Dissolution starts at the front of the propagating solvent. If for some reason a small region of porous medium has porosity which is slightly higher than elsewhere in the medium, then the local permeability will also have a large value in that region. Thus, based on Darcy's law, the discharge of reactive fluid in that region is also larger. This means that in this region the alteration front is locally more advanced. As time passes, this more advanced reaction zone grows faster and it produces a finger shape form in the porosity domain [12,18].

Reaction infiltration instability has been also observed in mantle rocks. It is described by the dissolution of rock (e.g., clinopyroxene) into the basaltic melt which leads to increased porosity and permeability. As melt migrates towards lower pressure, the solubility of rock increases and produces a solubility gradient. Thus melt transport is enhanced further by the dissolution. This process leads to the presence of instability, in the same way as the feedback mechanism for the dissolution front described in the above paragraph [1]. Thus, the governing equations of fingering instability in porous media can be also used to describe the melt channeling instability. Following Aharonov's study (1995), we employ the in-situ leaching equations as the governing equations [11]. The chemical transport is controlled by the kinetics of surface reaction, and then the general form of the mass transport equation in porous media can be written as [13]:

$$\phi_{,t} = (\phi K(\phi) h_{,i})_{,i} \quad (1)$$

$$v_i = -K(\phi) h_{,i} \quad (2)$$

$$(\phi C)_{,t} = (-\phi C v_i + \phi D_{ij} C_{,j})_{,i} + (\rho_s / \rho_f) N \psi \phi_{,t} \quad (3)$$

$$\phi_{,t} = k(\phi_{final} - \phi_{initial})^{1/3} (\phi_{final} - \phi)^{2/3} C \quad (4)$$

where in these equations, C is the concentration of reagent, v_i is the fluid/melt velocity and D is the diffusion coefficient. ϕ represents the porosity which can be linked to concentration through Eqn.(4). ϕ_{final} shows the final porosity of the porous medium, ρ_s and ρ_f are the density of solid and fluid respectively, N represents the stoichiometric coefficient, ψ is the ore grade and k is a rate constant. In real soils and rocks, the permeability K varies with porosity [13,14]:

$$K(\phi) = K_0 (\phi / \phi_0)^3 \quad (5)$$

2.2. Melt transport governing equations

The governing equations of melt movement and the matrix of a partially molten material have been given by McKenzie (1984). The equations were obtained from the conservation of mass, momentum, and energy using expressions from the theory of mixtures [4]. From the equations for conservation of melt and matrix mass we can write:

$$\phi_{,t} + v_k \phi_{,k} = (1 - \phi) v_{k,k} \quad (6)$$

We assume that the pressure is sufficient to support the weight of the overlying partially molten material. The equation governing the difference in the velocity of the melt and matrix is a modification of Darcy's law:

$$v_{k,k} = \left(\frac{K(\phi)}{\eta^f} p_{,j} \right)_{,j} \quad (7)$$

where η_f and p are the fluid viscosity and fluid pressure respectively. The permeability in this problem is linked to porosity using the Black-Kozeny-Karmen equation with the specific choice of parameters as proposed by McKenzie(1984) [4]:

$$K(\phi) = \frac{\phi^3 a^2}{1000(1 - \phi)^2} \quad (8)$$

where a is constant obtained from experiments. The stress equilibrium equation for viscous rock is written as:

$$\left(\eta (v_{i,j} + v_{j,i}) + \left(\eta_B - \frac{2}{3} \eta \right) v_{k,k} \delta_{ji} \right)_{,j} - p_{,i} = 0 \quad (9)$$

Here η_B is the bulk viscosity. The viscosity η is related to porosity and melt velocity by:

$$\eta = \eta_0 e^{-\alpha(\phi - \phi_0)} \left(\frac{\dot{\gamma}}{\dot{\gamma}_0} \right)^{1/n-1} \quad (10)$$

where $\dot{\gamma}_0$, n and α are material constants. $\dot{\gamma}$ is the second invariant of the incompressible component of the strain rate tensor:

$$\dot{\gamma} = \sqrt{\frac{(v_{i,j} + v_{j,i})^2}{2}} \quad (11)$$

The equations (6)–(10) represent a system of nonlinear, coupled partial differential equations for the variables v , ϕ and p . A strategy how to solve these equations is described in the next section.

3. Escript and Solution Algorithm

Escript is a non-linear, time-dependent partial differential equations (PDEs) modeling environment. It is written based on the programming language Python. One advantage of “escript” is that it is designed especially to solve partial differential equations and at the same time to provide an easy-to-use environment to develop and solve coupled models like the examples in this paper. This ability can be used efficiently in very large projects as it provides a clearer structure for the code, separating modeling issues from low-level numerical and computational performance issues. For a system of PDEs which has a solution with several components the PDE gets the form

[15]:

$$-\left(A_{ijkl}u_{k,l}\right)_{,j} - \left(B_{ijk}u_k\right)_{,j} + C_{ijk}u_{j,k} + D_{ij}u_j = Y_i - X_{ij,j} \quad (12)$$

where, A, B, C, D, Y and X are all data objects from different ranks in the domain. The natural boundary condition is introduced with this form:

$$-n_j \left(A_{ijkl}u_{k,l} + B_{ijk}u_k - X_{ij,j}\right) = y_i \quad (13)$$

where n_j is the outer normal field of the domain boundary and y_i is a given function. To give a value r_i to unknown vector-valued function u_i on certain locations of the domain, the below equation can be used:

$$u_i = r_i \text{ where } q_i > 0 \quad (14)$$

where q is a rank-1 characteristics function of the location where r_i applied. Now, inspecting the governing equations (Eqn.(1) to Eqn.(5)) and (Eqn.(6) to Eqn.(10)), we can easily identify the values for the PDE coefficients needed to calculate variables in each problem only by comparing the governing equations with Eqn(11). The two problems in this research are both coupled and non-linear.

In the fingering instability problem, the fluid flow equation is coupled with the chemical reaction term. Here the reactive transport equation is solved using the initial values in the first time step. The concentration which is obtained from this solution is then used to update the value of porosity, permeability and also fluid pressure for the next time step. In order to deal with numerical difficulties related to the advection term in the reactive transport equation, it is split and solved in two half time steps.

The principal non-linearities in the mantle transport governing equations arise from the constitutive relations between K, η, θ and γ . Here, the permeability is modeled as a simple power law with n in the range between 2 and 5. The solid shear viscosity η is strain-rate dependent and has been shown experimentally to be porosity weakening [16,17]. The initial value for pressure is introduced to Darcy's equation, and as the outcome a new set of values for the velocity field is obtained. The new value for melt velocity updates the porosity field and also the viscosity field on the domain in the next time step. As an example, the lines below show how equations (8) to (11) are solved in order to obtain a new value for velocity:

```
#####Velocity#####
from esys.escript import *
from esys.escript.linearPDEs import LinearPDE
x=mydomain.getX()
mypde=LinearPDE(mydomain)
g=util.grad(v)
Dij=(1./2.)*(g+transpose(g))
gamma_dot=util.sqrt(2)*util.length(Dij)
vis_bulk=2*vis_initial/(po**3)
k=(po**3)*(a**2)/(1000*((1-po)**2))
for i in range(mydomain.getDim()):
    for j in range(mydomain.getDim()):
        c[i,i,j,j]+=(vis_bulk-(2/3))*vis
        c[j,i,j,i]+=(vis)
        c[j,i,i,j]+=(vis)
sigma0=(pressure_last)*kronecker(mydomain)
mypde0.setValue(A=c,X=sigma0,q=msk,r=p_velocity)
v=mypde0.getSolution()
```

where po is porosity, msk is the boundary condition and $p_velocity$ represents the prescribed velocity.

4. Numerical Examples

4.1. Infiltration instability (fingering)

We assume the domain contains two interacting phases: untouched solid (rock) and fluid (melt). Melt is produced due to dissolution of rock and there is also mutual dependency between porosity and concentration. Thus once the reaction zone develops, the porosity is increased. The reaction front is unstable and as a result finger-like structures or channels with higher melt content form. We expect to see the enlargement of the reaction infiltration instability as time progresses. To numerically simulate the problem, we define a rectangular 2D domain (Fig.1) with uniform initial zero concentration all over the domain for the first time step. The initial value for porosity is set to be $\varnothing = \varnothing_{initial}$. The domain size has been chosen similar to other studies on the instability problem [18]. The domain meshes are 3000 linear triangular elements. On the top boundary we assume a prescribed velocity and a reference fluid pressure ($p > 0$). The fluid pressure value on the top boundary will cause a pressure gradient in the domain which leads to melt flow towards the lower domain line. Now we define a small harmonic deviation from $\varnothing = \varnothing_{final}$ on the top boundary ($x=13$) as a perturbation. The harmonic deviation is assumed to be a sine wave with frequency equal to 6. Figure 1 shows how the initial advanced porosity in early time steps leads to producing finger shape instability in later time steps of the solution.

Figure 2 shows the porosity fingering instability in a 3D domain. A uniform zero concentration for the first time step was defined all over the domain. A random three-dimensional function for initial porosity was defined on the bottom surface. The fluid pressure was considered to be slightly higher on the bottom surface. Variation of initial porosity value on the bottom surface leads to formation of finger-shape instabilities. The rough surface in Figure 2 is due to these fingering instabilities. Such a form for rocks can be seen in Nature.

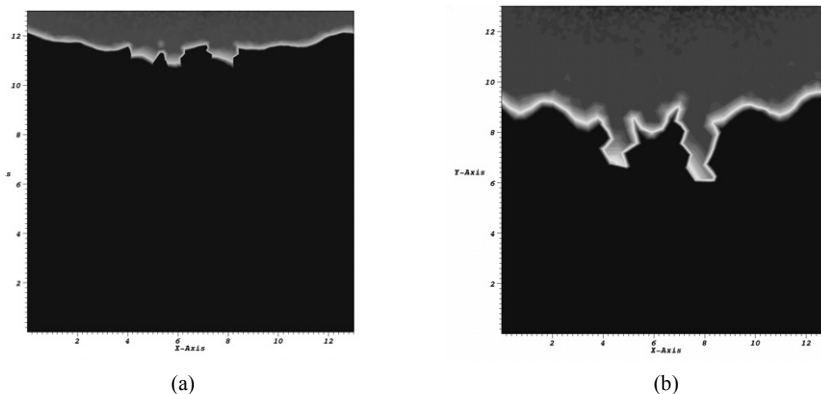


Fig. 1. 2D Fingering instability in (a) an early time step; (b) a late time step

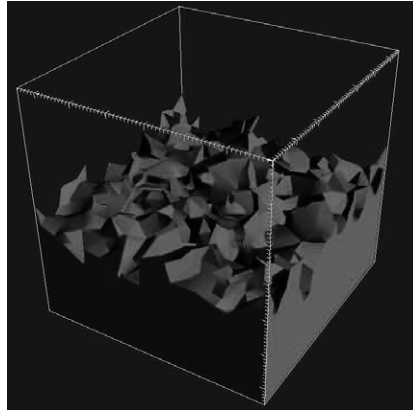


Fig. 2. Three-dimensional porosity fingering model

4.2. Shear localization and melt bands

To further investigate stress-driven melt segregation and organization, we employ our code for a series of simulations in a 2D viscoelastic domain subject to simple shear. For boundary condition, we assume that the problem is periodic in x direction. The permeability on the boundary is set to be zero. This results in making the pressure in the buffer cells irrelevant to the rest of the calculations. We define an initial white noise with random initial variations for the background porosity with various values of $n=1, 3$ and 5 .

In Figure 3, the distribution of viscosity on the domain is shown in the first and last time step when $n=5$ and the domain is at a strain of 300%. Figure 4 shows that the porosity field is distributed in bands of enhanced and depleted porosity. Similar to some other studies the bands are at an approximate angle of 20 degree [2,3,8]. The melt bands in red are roughly perpendicular to the axis of maximum extension rate and show the orientation of melt bands expected for a Newtonian viscosity, which tend to point away from the ridge axis. Moreover, melt bands point towards the ridge axis. Reducing n to 1 will lead to the melt bands growing more slowly than the fastest growing mode of linear theory.

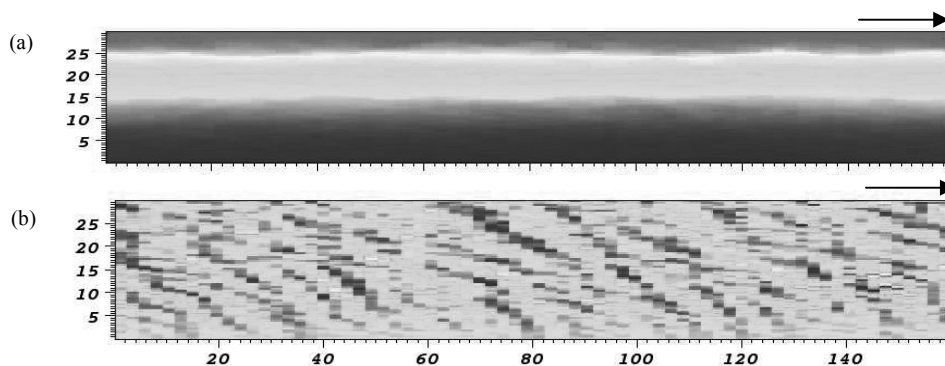


Fig. 3. Distribution of viscosity for a 2D domain subjected to simple shear: (a) the first time step; (b) the last time step.

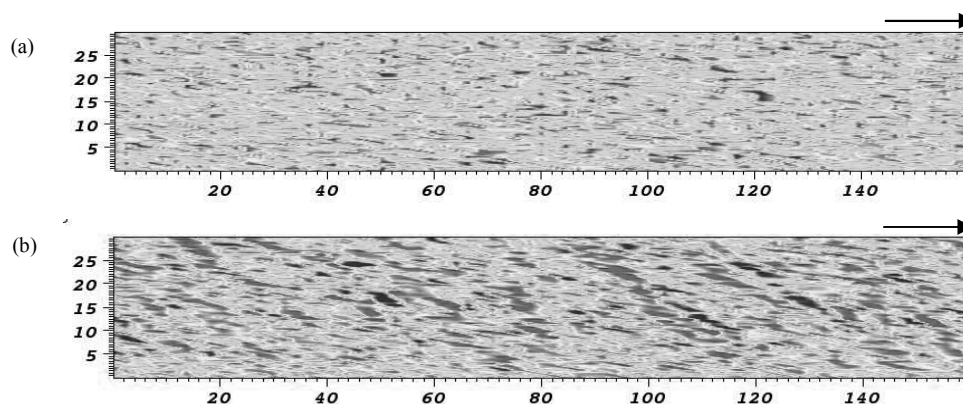


Fig. 4. Porosity distribution and melt bands in a 2D domain subjected to simple shear: (a) the first time step; (b) the last step

5. Conclusions

The results obtained in this study have implications for magma transport in the mantle, for example beneath mid-ocean ridges. The observations from mid-ocean ridges show that the oceanic crust is formed within 10 km of the ridge axis, whereas melt production is believed to occur over a region extending about 100 km from the axis. This implies some mechanism of melt focusing and distribution toward the axis of mid-ocean ridges. The infiltration instability (fingering instability) and melt-band-forming instability which were investigated in this research contribute to melt focusing along with some other mechanisms that have been proposed.

Numerical modeling was the tool employed in this study to provide better understanding of the melt segregation problem. A code was written for each scenario using the FEM coding environment “escript”. The advantage of “escript” is that it is specifically designed to solve partial differential equations (PDEs) and also it is capable of simulating problems from small to very large scales.

The first code successfully applied a finite element non-linear reactive diffusion-advection model to the porosity fingering instability problem in 2D and 3D. The infiltration instability or porosity fingering showed the importance of porosity feedback on stability of the reaction front. The positive feedback is due to porosity dependency of permeability. The solution increases the porosity and also the permeability. The porosity feedback causes instability of the initial straight reaction fronts. This instability and evaluation of porosity leads to finger shape distribution of porosity on the domain.

The second code was successful in solving the governing equations of melt transport by McKenzie (1984) in order to investigate the formation and orientation of melt bands. The outcomes of the FEM simulation showed that, as for flow beneath a mid-ocean ridge, the molten aggregates deformed in simple shear develop localized melt bands of high porosity and enhanced strain. These bands emerge at low angles to the plane of shear for a range of strain rates and stresses, and persist at low angles even after large shear strains.

Acknowledgements

We would like to acknowledge support from the ARC Discovery Grant DP0985662 and DP110103024 and also ongoing support through Auscope/NCRIS.

References

- 1 D.L. Kohlstedt and B.K. Holtzman, Annual Review of Earth and Planetary Sciences. 37 (2009) 561.
- 2 B.K. Holtzman and D.L. Kohlstedt, Jour. of Petrol. 48 (2007) 2379.

3. B.K. Holtzman, N. Groebner, M. Zimmerman, S. Ginsberg and D.L. Kohlstedt, *Geochem. Geophys. Geosyst.* 4 (2003). Art. No. 8607.
4. D. McKenzie, The Generation and Compaction of Partially Molten Rocks, *J Petrol.*, 25 (1984) 713.
5. J. Weertman, *J. Geophys. Res.* 76 (1979) 1171.
6. J.L. Ahern and D.L. Turcotte, *Earth Planet. Sci. Lett.* 445 (1979) 115.
7. D.J. Stevenson, *Geophys. Res. Lett.* 16 (1989) 1067.
8. R. Katz, M. Spiegelman and B.K. Holtzman, *Nature* 442 (2006) 676.
9. M.J. Daines and D.L. Kohlstedt, *J. Geophys. Res.* 102 (1997) 10257.
10. E. Aharonov, M. Spiegelman and P. Kelemen, *J. Geophys. Res.* 102 (1997) 14821.
11. E. Aharonov, J.A. Whitehead, M. Spiegelman and P. Kelemen, *J. Geophys. Res.* 100 (1995) 20433.
12. P. Ortoleva, E. Merino and C. Moore, *American Journal of Science*, 287 (1987) 979.
13. J. Liu and B. H. Brady, *Geotechnical and Geological Engineering*. 22 (2004) 1573.
14. H. B. Muhlhaus, J. Liu and B.E. Hobbs, *Modeling of In-situ Solution Mining Processes. Solid Mechanics and Its Applications. Springer Netherlands*, 87 (2001) 301-306.
15. L. Gross, H. Mühlhaus, E. Thorne and K. Steube, *Pure and Applied Geophysics*. 165 (2008) 653.
16. G. Hirth and D. L. Kohlstedt, *J. Geophys. Res.*, 100 (1995) 15441.
17. S. Mei, W. Bai, T. Hiraga, and D. Kohlstedt, *Earth Planet. Sci. Lett.*, 201 (2002) 491.
18. H. B. Muhlhaus, B.E. Hobbs, R. Freij-Ayoub and A. Ord, *Multi scales in rock alteration and ore deposit genesis. Proceedings of the 5th international workshop of bifurcation and localisation theory in geomechanics, Perth (1999) 355.1. S. Scholes, Discuss. Faraday Soc. No. 50 (1970) 222.*